Geophysical Research Letters

RESEARCH LETTER
10.1029/2019GL082694

# Rate-and-State Model Casts New Insight into Episodic Tremor and Slow-slip Variability in Cascadia

**Yingdi Luo**[1,2] and **Zhen Liu**[2]

[1]JIFRESSE, University of California, Los Angeles, CA, USA, [2]Jet Propulsion Laboratory, California Institute of Technology, Pasadena, CA, USA

**Key Points:**
- Episodic Tremor and Slow-slip (ETS) in Cascadia subduction zone occurs semi-regularly and shows intriguing spatio-temporal variability
- Rate-and-state subduction zone model with heterogenous frictional properties and stress conditions reproduces ETS in Cascadia
- Pore pressure variation can play a crucial role in affecting fault behaviors and can lead to observed ETS variabilities

**Supporting Information:**
- Supporting Information S1

**Correspondence to:**
Y. Luo,
luoyingd@jpl.nasa.gov

**Citation:**
Luo, Y., & Liu, Z. (2019). Rate-and-state model casts new insight into episodic tremor and slow-slip variability in Cascadia. *Geophysical Research Letters*, *46*, 6352–6362. https://doi.org/10.1029/2019GL082694

Received 4 MAR 2019
Accepted 20 MAY 2019
Accepted article online 28 MAY 2019
Published online 17 JUN 2019



**Abstract** Advances in geodetic and seismic observations have led to the discovery of Episodic Tremor and Slow-slip (ETS). ETS in Cascadia subduction zone occurs semiregularly and shows intriguing spatio-temporal variability reportedly associated with frictional properties and stress conditions. Yet the origin of complex ETS behaviors remains largely unknown. Here we develop a laboratory-based rate-and-state asperity-in-matrix subduction fault model, supported by geological observations of exhumed fault with heterogeneous frictional properties and pore pressure variation, to reproduce all ETS variability in good agreement with observations. Our results show that differential pore pressure plays a crucial role in affecting fault behaviors. Regions of asperities with decreased pore pressure tend to have increased tremor. Our study suggests that ETS variability can be used to probe otherwise enigmatic fault zone properties.

**Plain Language Summary** The discovery of slow earthquakes has greatly broadened our view of faulting processes and earthquake dynamics. The Episodic Tremor and Slow-slip (ETS) is one kind of slow earthquakes featuring slow-slip (fault moves very slowly yet still higher than plate motion, emitting no seismic signals) and accompanying tremors (weak, nonimpulsive, and continuous "humming" of fault). Intriguing ETS behaviors have been observed in Cascadia subduction zone such as broad-scale segmentation and local transient features including rapid tremor reversals, ETS "gap," and "halt." But physical explanation of these complex ETS behaviors is elusive. In this study we propose a rate-and-state fault model consisting of a mixture of competent tremor asperities embedded in incompetent matrix with heterogenous pore pressure. For the first time we show that the broad spectrum of observed ETS complexity can be reproduced in a unified mechanical model. We find that the variation in pore pressure (thus effective normal stress) can play a crucial role in affecting various-scale fault behaviors. Our study provides new insights into the physics of slow earthquakes, suggesting that the observation of ETS variability can be a useful tool, when combined with numerical model, to probe otherwise enigmatic fault zone properties and stress conditions on the subduction megathrust fault.

## 1. Introduction

The advances in observational techniques of geodesy and seismology have led to the discovery of a diverse spectrum of fault slip behaviors including slow earthquakes such as slow-slip events (SSEs), nonvolcanic tremor, low-frequency earthquakes and very low frequency earthquakes (Peng & Gomberg, 2010). These slow earthquakes have distinctive scaling relations (Ide et al., 2007) and rupture characteristics different from conventional earthquakes. Tremor, low-frequency earthquakes and very low frequency earthquakes are often referred to as seismic slow earthquakes to reflect their seismic signature. Meanwhile, SSE represents very slow slip transient that does not radiate seismic energy and is usually detected by geodetic instruments (e.g., Global Navigation Satellite Systems). These slow earthquakes are typically observed near the seismic-aseismic transition zones of younger subduction zone faults, for example, Cascadia, Southwest Japan, and Mexican subduction zone (Beroza & Ide, 2011; Peng & Gomberg, 2010; Schwartz & Rokosky, 2007).

Among these younger subduction zones, the Cascadia subduction zone in particular has witnessed a rich set of slow earthquake behaviors, thanks to the dense seismic and geodetic networks, and advances in tremor and SSE detection algorithm. In particular, the discovery of Episodic Tremor and Slow-slip (ETS) events has changed our view of tectonic hazards and earthquake cycles (Dragert et al., 2001; Rogers & Dragert, 2003). ETS event, as its name indicates, features spatio-temporal concurrence of tremor and SSE and is episodic. ETS events in Cascadia subduction zone show large-scale (hundreds of kilometers) along-strike

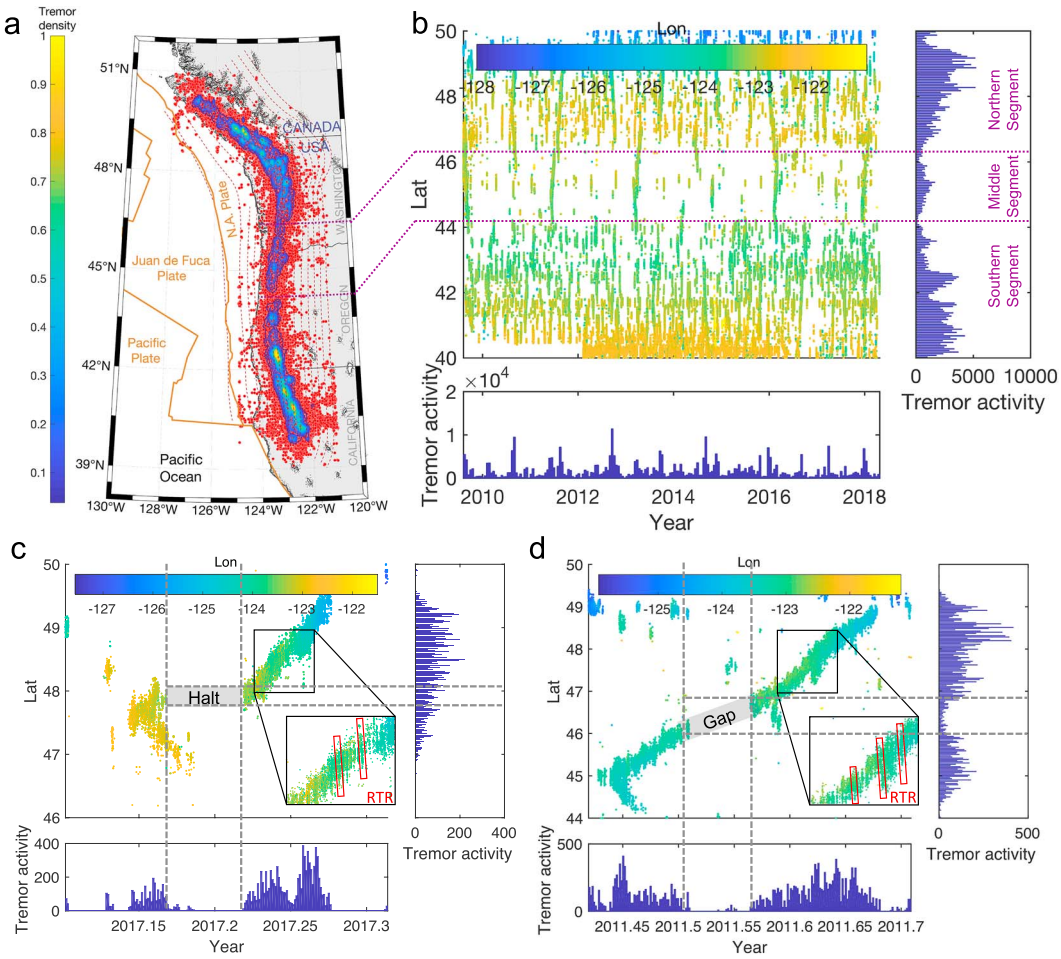


**Figure 1.** Space-time distribution of tremor along the Cascadia subduction zone. (a) Map view of tremor distribution from August 2009 to April 2018 along the Cascadia margin. The red circles are tremor location from PNSN tremor catalog (https://pnsn.org). The color contour shows normalized cumulative tremor density distribution. The brown curves are plate boundaries from PB2002 (Bird, 2003). The dark-red dashed lines indicate 5-km isodepth contour of plate interface (McCrory et al., 2012). **(b)** Spatiotemporal tremor distribution. The main figure shows the tremor catalog as a function of time (years) and location (latitude), color-coded by longitude. The Bottom and right plots are corresponding binned tremor activity as a function of time and location (latitude), respectively. There are clear three Episodic Tremor and Slow-slip (ETS) segments along the strike: the northern segment above lat. 46.4°N, the southern segment below lat. 44.2°N, and the middle segment in between. The ETS events in the middle segment have longer recurrence intervals and less overall tremor activities. The segment boundaries at about lat. 44.2 and 46.4° N have the lowest tremor activities but are not completely tremor-free. (c and d) Examples of local ETS variability of "Halt" and "Gap," respectively. The red rectangular boxes in the insets indicate cases of rapid tremor reversals, which propagate in the opposite direction of ETS at around 5 to 50 times faster propagation velocity than the forward migration. Note that in (d) ETS event nucleates at the center of the middle segment and propagates bilaterally along the strike. The south-going branch reaches the southern end of the middle segment and stops at about lat. 44°N. The north-going tremor branch reaches the northern end of the middle segment and stops approximately at lat. 46°N. But the underlying tremor-less SSE sustains its propagation with reduced propagation velocity. The tremor activity resumes in about 2 weeks further north (Bartlow et al., 2014; Figure S1). The ETS gap area near lat. 46°N seems present in multiple ETS events including the most recent 2018 event but is not completely tremor free. Tremor activity does occur in this gap region occasionally, although at much reduced level.

segmentations, which occurs semiregularly in each segment with various intervals from months to years (Figures 1a and 1b; Brudzinski & Allen, 2007; Wells et al., 2017). ETS events usually propagates steadily at several kilometers per day (Figures 1c and 1d; Houston et al., 2011) and can reach hundreds of kilometers along the strike. These events also display some intriguing behaviors at relatively smaller scales (tens of kilometers). Most notable features include the following (Figures 1c and 1d and Figure S1 in the supporting information):

1. ETS halt: ETS event propagates then pauses at certain location. It resumes roughly at the same location with days of delay. Figure 1c shows a typical ETS halt example in a 2017 ETS event in the northern segment of Cascadia.

2. ETS gap: ETS lacks of concomitant tremor activity at certain location and time during an event. The tremor activity then resumes at different location, roughly following the original ETS propagation direction but at reduced propagation velocity. Figure 1d shows a typical ETS gap example during the 2011 ETS event.
3. Rapid tremor reversals (RTRs): forward tremor migration sometimes accompanied by sparsely distributed backward propagation of tremors at much higher and near constant velocity, about 5-50 times faster than the forward migration (Figures 1c and 1d, inset; see also Houston et al., 2011).

Note that albeit ETS migration including RTRs that has been observed in Cascadia subduction zone shows predominantly near linear propagation, the ETS observed in Japan Nankai subduction zone sometimes show parabolic migration patterns instead, of which tremor propagation speed decays with propagation distance (e.g., Ando et al., 2012). It is also worth noting that in the situation like ETS gap, SSEs are observed without accompanying tremor activities (Figure S1; Wech & Bartlow, 2014), but not vice versa.

Significant efforts have been made over the past decades to model the physics of ETS (see Text S1 in the supporting information). But our understanding of ETS variability is still limited. One common feature in those models is very low effective normal stress in the seismic-aseismic transition region, presumably resulting from fluid overpressure (Hawthorne & Rubin, 2010). Previous studies show that SSE and tremor activities are sensitive to stress perturbations (Ide et al., 2007; Ito et al., 2007; Wech & Creager, 2011). There is strong correlation between tremor and tidal stress (Hawthorne & Rubin, 2010; Thomas et al., 2013). In addition, stress variation due to overlying faulting structures might exert control on ETS segmentations in Cascadia (Wells et al., 2017). Moreover, geological, laboratory, and theoretical studies indicate that pore pressure on a fault can vary significantly over different spatial and temporal scales as a result of sealing and unsealing due to permeability difference (Osborne & Swarbrick, 1997), fault valving (Sibson, 2014), porosity difference over the competent and incompetent materials as part of depth-dependent pressure-solution (Fagereng & Den Hartog, 2017), or fault gouging process (Luo, 2018). In addition to these, nontectonic loading such as tidal and/or hydrological forcing also affect stress conditions on a fault. Previous study shows that such stress variation can significantly influence SSEs due to their low stress nature (Luo & Liu, 2019; Wei et al., 2018). On the other hand, in the efforts of modeling tremor activities, Luo and Ampuero (Luo, 2018; Luo & Ampuero, 2011, 2018) developed an asperity-in-matrix model to reproduce the large-scale forward propagation and RTR in ETS events. The model is supported by geological observations of exhumed subduction fault zone materials composed of competent phacoid embedded in incompetent background matrix (*e.g.,* Fagereng et al., 2010). In their previous study they considered two end-member models that were able to reproduce observed large-scale features of ETS propagation with RTRs. In this study, we build on the previous modeling to combine geological constraints, ETS observation, and laboratory-based rate-and-state friction models to address two questions:

1. What physical processes could lead to the rich ETS variation in space and time?
2. What can we learn from ETS variability about fault zone properties and stress conditions that are crucial to faulting processes and large earthquake nucleation (*e.g.,* Galis et al., 2017)?

We show that local variations of differential pore pressure (thus effective normal stress and material strength) can be a viable mechanism to explain the broad spectrum of the observed ETS variability. In the next section we present the details of the method and model. We then present model results and discussion in the following sections.

## 2. Materials and Methods

### 2.1. Rate-and-State Friction Model

The numerical modeling of fault behaviors in this study follows the rate-and-state friction framework, derived from laboratory experiments (Dieterich, 1992; Ruina, 1983). The rate-and-state friction law has shown good success in modeling faulting processes from laboratory to natural earthquake scales (*e.g.,* Ampuero & Rubin, 2008). Under rate-and-state friction, fault is treated as frictional surface with shear stress $\tau$ equal to the product of effective normal stress $\sigma$ (fault normal stress minus pore pressure) and fault friction $\mu$

$$\tau = \sigma\mu \tag{1}$$

The fault friction coefficient $\mu$ is a function of slip rate $V$ and state $\theta$ and affected by constitutive parameters of direct and indirect effect $a$,$b$ and characteristic slip distance $D_c$:

$$\mu = \mu^* - a\ln\frac{V^*}{V} + b\ln\frac{V^*\theta}{D_c} \tag{2}$$

where $\mu^*$ is the reference friction coefficient and $V^*$ is the reference slip rate.

The state variable $\theta$ evolves with time and is normally described by laboratory-derived empirical evolution laws. In this study we adopt the "slip-law," which is most consistent with laboratory experiments (*e.g.,* Bhattacharya et al., 2015):

$$\dot{\theta} = -\frac{V\theta}{D_c}\ln\frac{V\theta}{D_c} \tag{3}$$

The constitutive parameters $a$,$b$ compete with each other and determine the material's property. When $a-b>0$, the material is velocity-strengthening (VS) as friction increases with increase of slip rate, and thus, fault is stable (no spontaneous rupture). When $a-b<0$, the material is velocity-weakening (VW) as it weakens (friction decreases) with increase of slip rate. Such VW fault could develop instability depending on its "criticalness." The criticalness of a VW fault is defined as whether it can generate spontaneous events, controlled by its size and corresponding frictional properties and stress conditions. Here we refer spontaneous events as self-activated sequences of slip transients without any external perturbation. For a homogenous fault, it will develop instability if it is "supercritical," of which the size of fault exceeds certain critical size $L_c$ determined by its frictional properties and effective normal stress $\sigma$, multiplied by a constant $C_g$ related to fault geometry:

$$L_c = C_g\frac{GD_c}{\sigma(b-a)} \tag{4}$$

where $G$ is the shear modulus of fault material.

The effective normal stress $\sigma$ is defined as the difference between normal stress and pore pressure. If the fault size is smaller than $L_c$, it is "subcritical" and no spontaneous event will occur albeit the fault being VW. For a heterogenous fault its stability is controlled by the same physical properties as in equation (4) but with more complicated forms (Luo & Ampuero, 2018) and the concept of "criticalness" still applies.

### 2.2. Subduction Zone ETS Modeled With Heterogenous Fault Properties

Previous research efforts have led to a number of ETS models with respective merits and limitations (see a detailed discussion of these models in Text S1). The asperity-in-matrix model is one of the most used models with a clear physical basis. The model considers the heterogenous subduction interface as a mixture of competent tremor-genic asperities embedded in the otherwise incompetent matrix (Figure 2a), and their interaction results in recurring ETS events. Such asperity-in-matrix model is supported by geological observations of exhumed subduction zone faults (Fagereng et al., 2010). Under the rate-and-state friction framework the competent tremor asperities are often modeled as VW patches and the incompetent matrix as VS materials. Such VW-VS mixed fault material (*e.g.,* Dublanchet et al., 2013*;* Skarbek et al., 2012*;* Yabe & Ide, 2018) has been used in previous studies (Luo, 2018*;* Luo & Ampuero, 2018) to generate the ETS event consisting of tremor, slow slip, and sparsely distributed RTRs.

Here we develop the baseline ETS model following the preferred Cascading model, in which ETS results from the interaction of tremor asperities and the background matrix from Luo (2018) with earthquake cycle simulator QDYN (Luo, Ampuero, Galvez, et al., 2017; Luo, Ampuero, Miyakoshi, & Irikura, 2017; see details in Text S2). In this cascading model tremor and SSE are the seismic and aseismic manifestation of the compound ETS event, respectively. The modeled ETS-genic region of the seismic-aseismic transition zone is simplified as 1-D linear fault along-strike embedded in a 2-D media. The fault width effect is handled through "1.5-D approximation" (see Text S3). The material of the VS background matrix strengthens with increase of slip rate to remain aseismic, while the scattered VW tremor asperities are simplified as single-cell patches with higher $b\sigma$ value than the background to be able to rupture

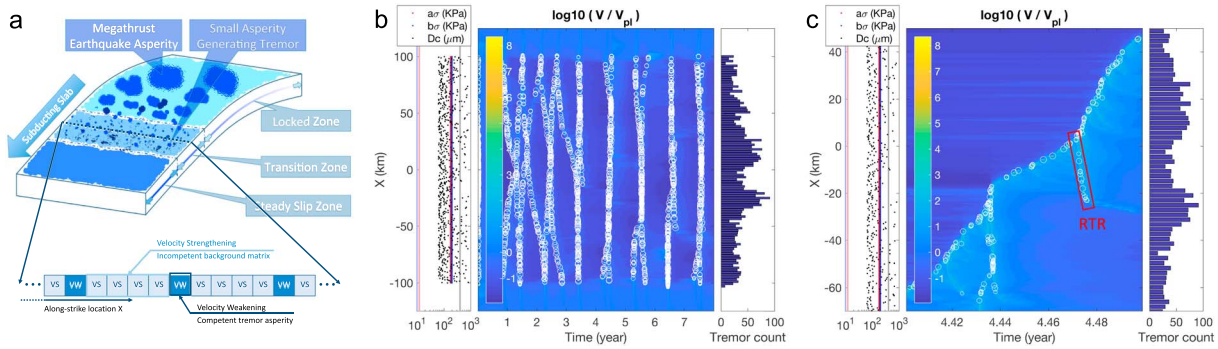


**Figure 2.** Schematic view of heterogeneous subduction zone model and baseline model ETS. (a) Model schematics: (top) seismic-aseismic transition region of subduction zone fault that hosts Episodic Tremor and Slow-slip (ETS) has numerous competent tremor asperities (dark colored) embedded in the incompetent background matrix (light colored). (bottom) In our rate-and-state model the transition zone is discretized as 1.5-D fault with alternating single-cell velocity-weakening (dark colored) tremor asperities and velocity-strengthening (light colored) background in the along-strike direction. (b) Modeled Cascadia multicycle ETS events: (left) model settings, red and blue dots: material strength $a\sigma$ and $b\sigma$, black dots: characteristic slip distance $D_c$, lighter color shows the corresponding value of the background matrix (velocity-strengthening part), while darker color is of the tremor asperities (velocity-weakening part). Note the high heterogeneity of $D_c$ value of the tremor asperities and the different strength between the asperities (higher value) and the background. (middle) Multicycle simulations of ETS events as a function of time (year) and along-strike location (km). The background color shows logarithmic slip rate normalized by tectonic loading rate. The white circles are detected tremor occurrence with circle size scaled with peak slip rate. Note that the first several (warm-up) ETS events are more chaotic due to initial conditions and are discarded. (right) The 2.5-km-binned tremor activity over all the computed ETSs. (c) Example of ETS (zoom-in of b) used as baseline model to test the effects of local stress variation. Example of RTR is indicated by red rectangular box.

seismically (Figure 2a). All tremor asperities are subcritical (with size smaller than $L_c$) via heterogenous and stochastic $D_c$ assigned to each asperity. Despite the asperities being individually subcritical, the bulk property of asperities and the background can be collectively supercritical thus allow spontaneous generation of recurring ETS (Luo & Ampuero, 2018). This composite fault model with mixed VW-VS rheology is physically realistic (Fagereng et al., 2010; Fagereng & Den Hartog, 2017; Osborne & Swarbrick, 1997; Rittenhouse, 1971; Sibson, 2014; Sibson, 2017) and supported by geological observations and numerous modeling efforts (*e.g.,* Luo & Ampuero, 2018*;* Yabe & Ide, 2018).

In this study we focus on northern Cascadia ETS. The model domain is 250 km along-strike. The center 200 km of the fault has VW tremor asperities embedded in the VS background. On both ends of the fault we impose 25-km pure VS (no asperities) edge to mitigate the effects of periodical boundary; the model domain size is comparable to the along-strike length of ETS segments in Cascadia. In our previous study (Luo, 2018) we have systematically studied such heterogenous VW-VS fault model with various ratio of VW and VS materials, frictional properties, and stress conditions. We find that the spacing (density) of tremor asperities and the overall effective normal stress of the fault can jointly affect the collective behaviors of the fault. Given fixed contrast of effective normal stress between the tremor asperities and the background (relative strength), if the tremor asperities are too far away from each other, the fault will be collectively subcritical and spontaneous events (tremor or SSE) will not sustain. With decreasing of asperity spacing fault can become more and more active and eventually the entire fault will rupture seismically. In this study, we base on the knowledge gained from previous studies to guide our tuning of these parameters to reproduce the ETS patterns that are consistent with observations of the northern Cascadia ETS (*e.g.,* Houston et al., 2011*;* Wech & Creager, 2011). The VS background matrix is set to have a low effective normal stress $\sigma$ of 1 MPa so it ruptures aseismically as SSE (*e.g.,* Liu & Rice, 2007). The single-cell VW tremor asperities have higher effective normal stress (20 MPa in the baseline model) so they can rupture more seismically (faster peak slip rate) and emit seismic signals to be detected as tremor. These tremor asperities are evenly spaced every five cells within the VS background (Figure 2a), which is around the middle of parametric spacing generating ETS. The tremor asperities have stochastic $D_c$ distribution resulting in a uniform distribution of asperity criticalness $dx/L_c = 0.02$ *to* 0.6 ($dx$ is the size of tremor asperity; Figures 2b and 2c, left panel, see also detailed parameter settings in Table S1 in the supporting information). All asperities are individually subcritical so they only break collectively while interacting with the background matrix reproducing episodic tremor (from asperities) and SSEs (from matrix). Note that to reduce computation cost we intentionally set all the tremor asperities to be subcritical so they will not break individually between ETS episodes. Allowing background

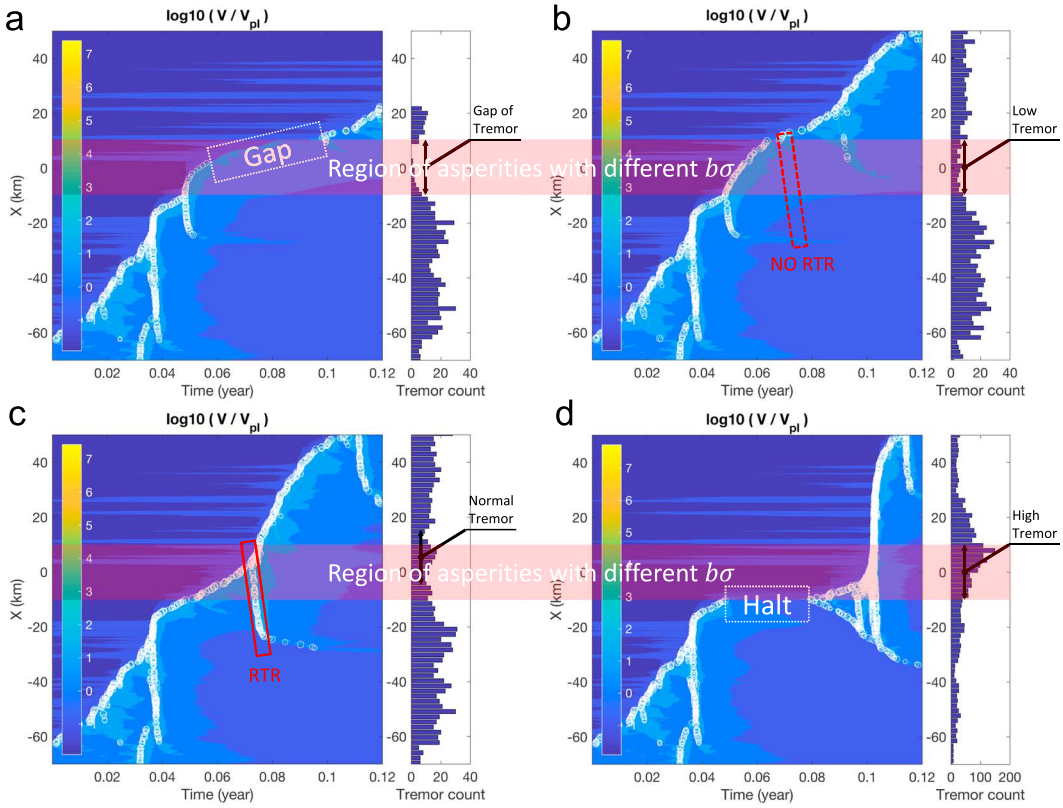


**Figure 3.** Modeled Episodic Tremor and Slow-slip (ETS) variability. Rate-and-state simulations of northern Cascadia ETS based on the "baseline" model, with a 20-km variation region at center (marked with horizontal red strip) of asperities with different effective normal stress. Similar panel layout as Figure 2b subpanel on the right indicates the 2.5-km-binned tremor activity during each ETS. (a) $R_b$=5. The variation region of asperities with lowest effective normal stress displays "ETS gap," where tremor activity is absent in the gap region. (b) $R_b$=10. The variation region of asperities with low effective normal stress shows low tremor activity. ETSs occur without RTR. (c) $R_b$=20. Same as reference model (Figure 2c) but with higher temporal resolution (denser time series output); thus, more tremor activities have been captured. The variation region of asperities with moderate effective normal stress witnesses ETS with RTR. (d) $R_b$=40. The variation region of asperities with high effective normal stress shows increased tremor activity and "ETS halt."

tremor activities will not change the results and we leave the study of such background tremor activities to a future study. Our model settings have taken into account previous studies, available field, laboratory and numerical results, and geodetic and seismic observations. In particular, our models are able to reproduce recurrent ETS (Figure 2b) with a recurrence interval of approximately 1 year and ETS duration close to 1 month (Figure 2c). The average propagation velocity of the forward ETS migration is about 5 km/day and sparsely distributed RTRs propagating backward about several to tens of times faster than the forward migration. All these are in good agreement with real-world observations in northern Cascadia (Houston et al., 2011). Note that the large-scale ETS propagation shows approximately linear pattern; at smaller scale the forward tremor migration instead shows parabolic pattern after each RTR, of which the ETS propagation speed decreases with distance (Figure 2c, see also Figure 3), consistent with Ando et al.'s (2012) hypothesis that large-scale ETS linear propagation could be superimposing of sequences of parabolic tremor bursts. In addition, albeit the RTRs shown in Figure 2c display mostly linear propagation pattern, the same simulation with a denser temporal output (Figure 3c) capturing tremor activities with improved temporal resolution displays the "slowdown" of RTR propagation similar to the parabolic RTR.

In this study we use a simple velocity threshold $V_{\mathrm{th}}$ to define tremor activities. If the slip rate of tremor asperity exceeds $10^4$ times the plate loading rate $V_{\mathrm{pl}}$, we classify it as a tremor activity. This definition is different from the conventional seismological definition of tremor, which is discriminated from seismic signals observed. However, given the small size of the source we considered and general view about tremor generation (e.g., Ando et al., 2012; Ariyoshi et al., 2012), we consider it a good first-order approximation.

For comparison the typical slip rate of modeled SSE, as the aseismic slip part of modeled ETS (e.g., Figure 2 c), is approximately equal to or small than 100 $V_{pl}$. Different $V_{th}$ values have been considered, and we find that it mostly only affects the number of detected tremor activities but not the overall pattern of tremor migration. This "Baseline Model" ETS that is in good agreement of observed large-scale ETS patterns in Cascadia is used to study the effect of local stress variation and how it affects the ETS behaviors in the next section. To mitigate the effect of initial conditions, we discard the first several ETS events and use ETS event occurred at the year 4 (Figure 2c).

## 3. Results

One important result from our previous efforts of ETS modeling is that the recurrence intervals of ETS is approximately proportional to the effective normal stress (*e.g.,* Luo, 2018*;* for SSE see Liu & Rice, 2007), suggesting that the ETS process is stress-sensitive. Studies of SSEs also shown that they are prone to stress perturbations due to their low stress drop nature (Luo & Liu, 2019*;* Wei et al., 2018). To investigate whether and how stress variations at local scale can affect small-scale ETS variabilities such as tremor gap, halt, and RTRs, we introduce variations of effective normal stress on part of the fault ("variation region"). In particular, right before the onset of the baseline model ETS, we vary the material strength associated with indirect effect, defined as $b\sigma$, of asperities in a 20-km variation region at the center of the fault between along-strike location X = (-10, +10) km. We also change the material strength associated with direct effect $a\sigma$ proportionally to maintain the $a/b$ ratio of the asperities fixed. Since the effective normal stress $\sigma$ equals to fault normal stress minus pore pressure, high pore pressure reduces effective normal stress when fault normal stress maintains the same. The $\boldsymbol{b\sigma}$ ratio between the asperities in the variation region and the background, which we define as relative strength $R_b = (b\sigma)_{aspv}/(b\sigma)_{bg}$, is varied from 1 to 40, as compared to the value of 20 in the baseline model. The relative strength represents how easy an embedded asperity is ready to break (Luo & Ampuero, 2018); asperity with larger relative strength is "stronger" that is harder to break and emits more energy while breaking. By varying the relative strength alone, our models are able to reproduce the full spectrum of the observed ETS local variabilities including ETS gap, halt, and RTRs (Figure 3). In particular, we find the following:

1. Region of asperities with the lowest relative strength (highest pore pressure, approximately $R_b$<8) displays "ETS gap" behavior, where tremor activities temporarily pause while (tremor-less) SSE continues propagating and eventually tremor resumes (at X>10 km; Figure 3a).
2. Region of asperities with relatively low relative strength (high pore pressure, approximately 8<$R_b$<15) shows reduced tremor activity and no RTR (Figure 3b).
3. Region of asperities with moderate to high relative strength (moderate pore pressure, approximately $R_b$ >15) will have ETS events with RTRs (Figure 3c), consistent with observations that RTRs are only sparsely distributed during the ETS episode.
4. Region of asperities with increasing relative strength (decreasing pore pressure) will have increasing tremor activity, faster propagating ETS, and more RTRs. At approximately $R_b$>30, "ETS halt" starts to emerge, where tremor activities cease and later resume at the same location (Figure 3d). Note that in our rate-and-state model the ETS resumed after "ETS halt" shows a noticeable increase of tremor activity corresponding to the reactivation of ETS in the variation region with high relative strength, qualitatively agreeing with the observation in Cascadia (Figure 1c). Meanwhile, in our modal multiple RTRs are activated after the halt which is not observed, such discrepancy might be due to the simplification in our model, in which the fault is 2.5-D without along-dip variation, and the change of stress condition along-strike being abrupt rather than gradual inside and outside the variation region.

To verify the generality of the model results, we tested different scenarios by varying asperity density (fraction of tremor area versus total area) and overall relative strength inside and outside tremor asperities in more general model settings. These include consideration of different size of variation region at different locations on the fault, using other baseline ETS events generated in later cycles, and baseline ETS generated with different fault zone properties. We find that actual relative strength $R_b$ to reproduce the ETS variability depends on the baseline model settings, location, and dimension of the variation region, yet the general trend of tremor activity increase with asperity relative strength (decrease with asperity pore pressure) in the variation region remains the same; that is, ETS behavior changes from tremor-less "ETS gap" to low

tremor activity of ETS without RTRs, to high tremor activity of ETS with RTR, and to the highest tremor activity and "ETS halt" (e.g., Figures S2 and S3). In the case where the variation region becomes very large (approximately 40 km or larger), the "ETS gap" disappears and ETS stops, as the tremor-less SSE follows a parabolic decaying pattern, similar to postseismic slip of a failing VW patch in VS media (*e.g.,* Ampuero & Rubin, 2008). Thus, ETS can only resume within a limited distance (e.g., Figure S3a). It is also worth noting that nucleation of RTRs seems stimulated near the edge of the variation region, when ETS propagates from region with stronger asperities (higher $\sigma$) to weaker asperities (lower $\sigma$) but not vice versa (Figures 3a and 3b, S2a and S2b, and S3a and S3b).

The results from this simple and unified framework of local stress (strength) variation within the ETS region are in good agreement with the observations in Cascadia subduction zone. It is also supported by previous findings of strong correlation between local stress conditions and tremor/SSE activities (Hawthorne & Rubin, 2010; Wallace et al., 2018; Wells et al., 2017). The low effective normal stress in ETS zone (*e.g.,* Ide et al., 2007; Ito & Obara, 2006; Luo, 2018) suggests that the in situ pore pressure is close to the level of lithostatic stress, which approximates fault normal stress. Thus, changes in pore pressure can result in large variation in effective normal stress within the ETS zone which in turn affects the in situ criticalness of the region and affects macroscopic faulting behavior. Such variation can be induced by various sources such as fluid pressure waves (Mulargin & Bizzarri, 2015), seasonal hydrological loading (Johnson et al., 2017), or stress perturbation from tidal loading and/or tectonic processes such as earthquakes. Our results highlight the importance of quantifying these tectonic and nontectonic loading sources and their influence on the episodic ETS behaviors.

## 4. Discussions and Conclusions

Advances in understanding slow to fast earthquakes hinge on an interdisciplinary investigation through the integration of laboratory experiment, geophysics, geology and modeling studies (Bürgmann, 2018). In this study we combine seismological and geodetic observations of ETS, geological and mechanical inference of subduction zone fault heterogeneity with a laboratory derived rate-and-state friction modeling. Our asperity-in-matrix model incorporates heterogenous frictional properties and stress conditions, representing physically realistic subduction zone. By considering a common mechanism of stress (pore pressure) variations in a local region with multiple tremor asperities, the model is able to reproduce the broad spectrum of observed ETS variability.

Our modeling results can be explained in terms of heterogeneous frictional properties and interactions between tremor asperities and/or with the background matrix. The degree of readiness to generate spontaneous rupture event, the "criticalness" of a particular part of a fault can change with in situ stress level and display different macroscopic behaviors. Regions with low strength asperities can be locally "subcritical," that is, no spontaneous rupture if it is a stand-alone fault without any neighboring VW region (Figure 12 in Luo & Ampuero, 2018). When the region is very subcritical due to very low asperity strength, and/or the ETS event is weak, the region can act as a barrier to ETS propagation (Figure S3a). When the low stress region is slightly subcritical (due to moderately low asperity strength), the ETS can propagate with reduced velocity without emitting seismic signals (ETS gap; Figures 3a and S2a). The stress interaction between local low stress region and its high stress neighbors can sustain tremor-less ETS propagation for a limited distance. The low stress region will eventually become supercritical when it has increasing higher asperity strength facilitating relatively rapid (seismic) rupture of tremor asperities. For the regions of asperities with even higher strength, the resultant supercriticalness and high stress drop from tremor asperity rupture jointly contribute to the increase in tremor activities (Figures 3d, S2d, and S3d). The tremor asperities with high stress drop have stronger interaction with the VS background and neighboring asperities and also take longer to be loaded to reach failure, assuming the same loading rate, this is consistent with observations that acceleration of tremor migration is associated with energetic tremor of relatively high stress drop (e.g., Ando et al., 2012; Kano et al., 2018). The combination of heterogeneous frictional properties and the interactions of high stress drop asperities also promotes the development of sparsely distributed RTRs, as the elevated background slip rate of SSE tends to increase the propagation velocity of the backward tremor. If the asperities take too long to fail, then the heightened background slip rate may decrease to a level causing the ETS to halt, until the ETS resumes.

Our model is consistent with the observation that the tremor and SSE can be modulated by small stress perturbation such as tidal stress (Hawthorne & Rubin, 2010; Thomas et al., 2013). It also provides an explanation to the observed temporal variation of ETS. For example, recurrent individual ETS event can have different spatiotemporal tremor characteristics (Houston et al., 2011). Tremor gap in one ETS event can be fulfilled in another ETS. Occasionally ETS can propagate through the persistent segmentation boundary that is not completely tremor free (Figure 1). The combination of external stress perturbation from tectonic and nontectonic sources and stress change due to interaction between tremor asperities could continuously modify stress conditions on the plate interface, affecting the spatiotemporal variability of the observed ETS patterns.

Despite the model presented here focus on the small scale ETS variability in Cascadia, we expect that the model is applicable to a broader scale to explain more permanent ETS variation such as margin-parallel ETS segmentations if "semipermanent" stress variation exists at larger area on a longer time scale. For instance, the northern and southern segments of Cascadia subduction zone have similar ETS recurrence intervals (approximately 1 year) and comparable tremor activities, while the middle segment has a much longer recurrence interval. Wells et al. (2017) proposed that the upper plate block-boundary faults in Cascadia can extend to the overpressurized megathrust, damping generation of tremor, and related slow slip by forming fracture pathways to facilitate fluid escape thus reduce fluid pressure. Thus, the along-strike segmentation in ETS might reflect broader scale fluid variation (thus effective normal stress and relative strength variation) due to the crustal fault control.

Our model results also provide a potential way to probe fault zone properties and stressing conditions that are otherwise difficult to estimate. For example, the persistent ETS variation in space could shed light on the in situ fault zone properties. The similarity of ETS patterns in the northern and southern segments of Cascadia suggests that they are likely controlled by similar fault zone properties. Since ETS recurrence interval is approximately proportional to the overall effective normal stress, the much longer ETS recurrence interval in the middle segment may suggest that its bulk effective normal stress is much higher than other two segments. Since tremor activities increase with the relative strength of asperities, the overall lower tremor activity in the middle segment suggests the relative strength between tremor asperities and the background matrix has to be lower in the middle segment, possibly dictated by the combination of constitutive fault parameters and variation in effective normal stress $\sigma$. Similarly, the "barriers" between the northern, middle, and southern segments where the lowest overall tremor activities observed are likely related to the lowest relative strength in these regions, which can be controlled predominantly by higher pore pressure (thus lower $\sigma$) in asperities or lower pore pressure (higher $\sigma$) in the background matrix, or a combination of both, if other fault constitutive parameters are the same.

The time-dependent ETS variability may also provide important information about the evolution of fault stress conditions. By examining the time-dependent ETS variability and the relation with tectonic and nontectonic loading sources, we may gain the insight about the underlying cause of the observed change. For example, how do the sinusoid and nonsinusoid forcing from tectonic/nontectonic sources affect in situ stress conditions and ETS variability? What is the cumulative effect of the past ETS activity on future ETS event? Is there any systematic temporal change in ETS activities and what can it tell us about nucleation process of future Cascadia M9 megathrust earthquakes? Addressing these would require continuing study through laboratory-based modeling as we show here and combination with the constraints from seismological and geodetic observations.

The ETS events in Cascadia also show some intriguing patterns in along-dip direction. For example, tremor swarms propagate rapidly up-dip and down-dip of the subduction zone in the ETS region (e.g., Ghosh et al., 2012) , which may have similar mechanism as the RTRs we have modeled, and a gradual reduction of ETS recurrence intervals to a continuously creeping state with increasing depth (e.g., Wech & Creager, 2011) that is probably due to a gradual change of effective normal stress and frictional property. Studying those depth-dependent ETS behaviors with along-strike variation would require consideration of heterogenous frictional properties with 3-D stress variation. Our heterogenous rate-and-state asperity-in-matrix model with stress variation is one promising candidate to address such depth-dependent ETS variability. We are working to improve the modeling capability to tackle these 3-D problems in our future study with ultimate goal of providing insights into the relationship between ETS events and future megathrust earthquake.

**Acknowledgments**

This work was carried out at the Jet Propulsion Laboratory (JPL), California Institute of Technology, under a contract with the National Aeronautics and Space Administration. The authors declare that they have no competing interests. The tremor catalog used in this study and more detailed information is publicly available on PNSN website (https://pnsn.org). The rate-and-state earthquake simulator we used is available at the GitHub (https://github.com/ydluo/qdyn). Other materials in this study are available upon request.

## References

Ampuero, J. P., & Rubin, A. M. (2008). Earthquake nucleation on rate and state faults—Aging and slip laws. *Journal of Geophysical Research*, *113*, B01302. https://doi.org/10.1029/2007JB005082

Ando, R., Takeda, N., & Yamashita, T. (2012). Propagation dynamics of seismic and aseismic slip governed by fault heterogeneity and Newtonian rheology. *Journal of Geophysical Research*, *117*, B11308. https://doi.org/10.1029/2012JB009532

Ariyoshi, K., Matsuzawa, T., Ampuero, J. P., Nakata, R., Hori, T., Kaneda, Y., et al. (2012). Migration process of very low-frequency events based on a chain-reaction model and its application to the detection of preseismic slip for megathrust earthquakes. *Earth Planets Space*, *64*(8), 693–702. https://doi.org/10.5047/eps.2010.09.003

Bartlow, N. M., Wallace, L. M., Beavan, R. J., Bannister, S., & Segall, P. (2014). Time-dependent modeling of slow slip events and associated seismicity and tremor at the Hikurangi subduction zone, New Zealand. *Journal of Geophysical Research: Solid Earth*, *119*, 734–753. https://doi.org/10.1002/2013JB010609

Beroza, G. C., & Ide, S. (2011). Slow earthquakes and nonvolcanic tremor. *Annual Review of Earth and Planetary Sciences*, *39*(1), 271–296. https://doi.org/10.1146/annurev-earth-040809-152531

Bhattacharya, P., Rubin, A. M., Bayart, E., Savage, H. M., & Marone, C. (2015). Critical evaluation of state evolution laws in rate and state friction: Fitting large velocity steps in simulated fault gouge with time-, slip-, and stress-dependent constitutive laws. *Journal of Geophysical Research: Solid Earth*, *120*, 6365–6385. https://doi.org/10.1002/2015jb012437

Bird, P. (2003). An updated digital model of plate boundaries. *Geochemistry, Geophysics, Geosystems*, *4*(3), 1027. https://doi.org/10.1029/2001GC000252

Brudzinski, M. R., & Allen, R. M. (2007). Segmentation in episodic tremor and slip all along Cascadia. *Geology*, *35*(10), 907–910. https://doi.org/10.1130/G23740A

Bürgmann, R. (2018). The geophysics, geology and mechanics of slow fault slip. *Earth and Planetary Science Letters*, *495*, 112–134. https://doi.org/10.1016/j.epsl.2018.04.062

Dieterich, J. H. (1992). Earthquake nucleation on faults with rate-and state-dependent strength. *Tectonophysics*, *211*(1–4), 115–134. https://doi.org/10.1016/0040-1951(92)90055-b

Dragert, H., Wang, K., & James, T. S. (2001). A silent slip event on the deeper Cascadia subduction interface. *Science*, *292*(5521), 1525–1528. https://doi.org/10.1126/science.1060152

Dublanchet, P., Bernard, P., & Favreau, P. (2013). Interactions and triggering in a 3-D rate-and-state asperity model. *Journal of Geophysical Research: Solid Earth*, *118*, 2225–2245. https://doi.org/10.1002/jgrb.50187

Fagereng, Å., & Den Hartog, S. A. (2017). Subduction megathrust creep governed by pressure solution and frictional-viscous flow. *Nature Geoscience*, *10*(1), 51–57. https://doi.org/10.1038/ngeo2857

Fagereng, Å., Remitti, F., & Sibson, R. H. (2010). Shear veins observed within anisotropic fabric at high angles to the maximum compressive stress. *Nature Geoscience*, *3*(7), 482–485. https://doi.org/10.1038/ngeo898

Galis, M., Ampuero, J. P., Mai, P. M., & Cappa, F. (2017). Induced seismicity provides insight into why earthquake ruptures stop. *Science advances*, *3*(12), eaap7528. https://doi.org/10.1126/sciadv.aap7528

Ghosh, A., Vidale, J. E., & Creager, K. C. (2012). Tremor asperities in the transition zone control evolution of slow earthquakes. *Journal of Geophysical Research*, *117*, B10301. https://doi.org/10.1029/2012JB009249

Hawthorne, J. C., & Rubin, A. M. (2010). Tidal modulation of slow slip in Cascadia. *Journal of Geophysical Research*, *115*, B09406. https://doi.org/10.1029/2010JB007502

Houston, H., Delbridge, B. G., Wech, A. G., & Creager, K. C. (2011). Rapid tremor reversals in Cascadia generated by a weakened plate interface. *Nature Geoscience*, *4*(6), 404–409. https://doi.org/10.1038/ngeo1157

Ide, S., Beroza, G. C., Shelly, D. R., & Uchide, T. (2007). A scaling law for slow earthquakes. *Nature*, *447*(7140), 76–79. https://doi.org/10.1038/nature05780

Ito, Y., & Obara, K. (2006). Very low frequency earthquakes within accretionary prisms are very low stress-drop earthquakes. *Geophysical Research Letters*, *33*, L09302. https://doi.org/10.1029/2006GL025883

Ito, Y., Obara, K., Shiomi, K., Sekine, S., & Hirose, H. (2007). Slow earthquakes coincident with episodic tremors and slow slip events. *Science*, *315*(5811), 503–506. https://doi.org/10.1126/science.1134454

Johnson, C. W., Fu, Y., & Bürgmann, R. (2017). Seasonal water storage, stress modulation, and California seismicity. *Science*, *356*(6343), 1161–1164. https://doi.org/10.1126/science.aak9547

Kano, M., Kato, A., Ando, R., & Obara, K. (2018). Strength of tremor patches along deep transition zone of a megathrust. *Scientific reports*, *8*(1), 3655. https://doi.org/10.1038/s41598-018-22048-8

Liu, Y., & Rice, J. R. (2007). Spontaneous and triggered aseismic deformation transients in a subduction fault model. *Journal of Geophysical Research*, *112*, B09404. https://doi.org/10.1029/2007JB004930

Luo Y. (2018). Earthquake moment-area scaling relations and the effect of fault heterogeneity on slow to fast earthquake slip (*Doctoral dissertation, California Institute of Technology*). https://doi.org/10.7907/Z9SQ8XMV.

Luo, Y., & Ampuero, J. P. (2011, December). Numerical simulation of tremor migration triggered by slow slip and rapid tremor reversals. In AGU Fall Meeting Abstracts.

Luo, Y., & Ampuero, J. P. (2018). Stability of faults with heterogeneous friction properties and effective normal stress. *Tectonophysics*, *733*, 257–272. https://doi.org/10.1016/j.tecto.2017.11.006

Luo Y., Ampuero, J. P., Galvez, P., Van den Ende, M., & Idini, B. (2017). QDYN: A Quasi-DYNamic Earthquake Simulator (V1. 1). URL: https://github. com/ydluo/qdyn. https://doi.org/10.5281/zenodo.322459.

Luo, Y., Ampuero, J. P., Miyakoshi, K., & Irikura, K. (2017). Surface rupture effects on earthquake moment-area scaling relations. *Pure and Applied Geophysics*, *174*(9), 3331–3342. https://doi.org/10.1007/s00024-017-1467-4

Luo, Y., & Liu, Z. (2019). Slow-slip recurrent pattern changes: perturbation responding and possible scenarios of precursor toward a megathrust earthquake. *Geochemistry, Geophysics, Geosystems.*, *20*, 852–871. https://doi.org/10.1029/2018GC008021

McCrory, P. A., Blair, J. L., Waldhauser, F., & Oppenheimer, D. H. (2012). Juan de Fuca slab geometry and its relation to Wadati-Benioff zone seismicity. *Journal of Geophysical Research*, *117*, B09306. https://doi.org/10.1029/2012JB009407

Mulargin, F., & Bizzarri, A. (2015). Fluid pressure waves trigger earthquakes. *Geophysical Journal International*, *200*(3), 1279–1283. https://doi.org/10.1093/gji/ggu469

Osborne, M. J., & Swarbrick, R. E. (1997). Mechanisms for generating overpressure in sedimentary basins: A reevaluation. *AAPG bulletin*, *81*(6), 1023–1041.

Peng, Z., & Gomberg, J. (2010). An integrated perspective of the continuum between earthquakes and slow-slip phenomena. *Nature Geoscience*, *3*(9), 599–607. https://doi.org/10.1038/ngeo940

Rittenhouse, G. (1971). Mechanical compaction of sands containing different percentages of ductile grains: A theoretical approach. *AAPG Bulletin*, *55*(1), 92–96.

Rogers, G., & Dragert, H. (2003). Episodic tremor and slip on the Cascadia subduction zone: The chatter of silent slip. *Science*, *300*(5627), 1942–1943. https://doi.org/10.1126/science.1084783

Ruina, A. (1983). Slip instability and state variable friction laws. *Journal of Geophysical Research*, *88*(B12), 10,359–10,370.

Schwartz, S. Y., & Rokosky, J. M. (2007). Slow slip events and seismic tremor at circum-Pacific subduction zones. *Reviews of Geophysics*, *45*, RG3004. https://doi.org/10.1029/2006RG000208

Sibson, R. H. (2014). Earthquake rupturing in fluid-overpressured crust: how common? *Pure and Applied Geophysics*, *171*(11), 2867–2885. https://doi.org/10.1007/s00024-014-0838-3

Sibson, R. H. (2017). Tensile overpressure compartments on low-angle thrust faults. *Earth Planets Space*, *69*(1), 113. https://doi.org/10.1186/s40623-017-0699-y

Skarbek, R. M., Rempel, A. W., & Schmidt, D. A. (2012). Geologic heterogeneity can produce aseismic slip transients. *Geophysical Research Letters*, *39*, L21306. https://doi.org/10.1029/2012GL053762

Thomas, T. W., Vidale, J. E., Houston, H., Creager, K. C., Sweet, J. R., & Ghosh, A. (2013). Evidence for tidal triggering of high-amplitude rapid tremor reversals and tremor streaks in northern Cascadia. *Geophysical Research Letters*, *40*, 4254–4259. https://doi.org/10.1002/grl.50832

Wallace, L. M., Hreinsdottir, S., Ellis, S., Hamling, I., D'Anastasio, E., & Denys, P. (2018). Triggered slow slip and afterslip on the southern Hikurangi subduction zone following the Kaikōura earthquake. *Geophysical Research Letters*, *45*, 4710–4718. https://doi.org/10.1002/2018GL077385

Wech, A. G., & Bartlow, N. M. (2014). Slip rate and tremor genesis in Cascadia. *Geophysical Research Letters*, *41*, 392–398. https://doi.org/10.1002/2013GL058607

Wech, A. G., & Creager, K. C. (2011). A continuum of stress, strength and slip in the Cascadia subduction zone. *Nature Geoscience*, *4*(9), 624–628. https://doi.org/10.1038/ngeo1215

Wei, M., Kaneko, Y., Shi, P., & Liu, Y. (2018). Numerical modeling of dynamically triggered shallow slow slip events in New Zealand by the 2016 Mw 7.8 Kaikoura earthquake. *Geophysical Research Letters*, *45*, 4764–4772. https://doi.org/10.1029/2018GL077879

Wells, R. E., Blakely, R. J., Wech, A. G., McCrory, P. A., & Michael, A. (2017). Cascadia subduction tremor muted by crustal faults. *Geology*, *45*(6), 515–518. https://doi.org/10.1130/G38835.1

Yabe, S., & Ide, S. (2018). Variations in precursory slip behavior resulting from frictional heterogeneity. *Progress in Earth and Planetary Science*, *5*(1), 43. https://doi.org/10.1186/s40645-018-0201-x